Published in final edited form as:
Chem Biol. 2011 March 25; 18(3): 336–343. doi:10.1016/j.chembiol.2010.12.009.

Understanding the Structure/Activity Relationships of the Iron Regulatory Peptide Hepcidin

Richard J. Clark[1], **Chia Chia Tan**[1], **Gloria C. Preza**[2], **Elizabeta Nemeth**[2], **Tomas Ganz**[2], and **David J. Craik**[1]

[1] The University of Queensland, Institute for Molecular Bioscience, Brisbane, Queensland 4072 Australia

[2] David Geffen School of Medicine, University of California, Los Angeles, California, USA

Summary

The peptide hormone hepcidin is a key homeostatic regulator of iron metabolism and involved in pathological regulation of iron in response to infection, inflammation, hypoxia and anaemia. It acts by binding to the iron exporter ferroportin, causing it to be internalised and degraded; however, little is known about the structure/activity relationships of the interaction of hepcidin with ferroportin. Here we show that there are key residues within the N-terminal region of hepcidin that influence its interaction with ferroportin, and we explore the structure/function relationships at these positions. We found that the interaction is primarily hydrophobic with critical stereochemical requirements at positions 4 and 6. In addition, a series of hepcidin mutants in which disulfide bonds had been replaced with diselenide bonds showed no change in biological activity compared to native hepcidin. The results provide mechanistic insight into the interaction between hepcidin and ferroportin and identify important constraints for the development of hepcidin congeners for the treatment of hereditary iron overload.

Introduction

The peptide hormone hepcidin is a key regulator of iron homeostasis and is produced by the liver in response to high plasma iron levels and inflammatory stimuli (Ganz, 2008; Nemeth and Ganz, 2006). Ferroportin is the sole cellular iron exporter and is expressed on the surface of intestinal enterocytes, macrophages, hepatocytes and placenta where it releases cellular iron into the plasma (Donovan, et al., 2005). Hepcidin acts by binding to ferroportin, causing the transporter to be internalised and degraded (Nemeth, et al., 2004). The rate of iron efflux from these cells is proportional to the level of ferroportin on the cell membranes. Therefore, hepcidin-induced degradation of ferroportin results in a decrease in the circulating levels of iron within the body.

Hepcidin is synthesised as an 84 amino acid prepropeptide that is subsequently processed to the mature 25 residue peptide, which contains eight cysteines, linked to form four disulfide bonds (Figure 1) (Krause, et al., 2000;Park, et al., 2001). The connectivity of these disulfide bonds was originally proposed, based on a detailed NMR analysis, to be in a 7-23, 10-22,

Address correspondence to: Richard J. Clark, The University of Queensland, Institute for Molecular Bioscience, Brisbane, QLD 4072, Australia. Tel: 61-7-33462021. Fax: 61-7-33462101; r.clark@imb.uq.edu.au.

11-19 and 13-14 ladder-like arrangement that includes a rare vicinal disulfide bond (between Cys 13-14) (Hunter, et al., 2002). A later structural study on bass hepcidin reported the same disulfide connectivity (Lauth, et al., 2005). However, recently it has been shown, using NMR, disulfide mapping and X-ray crystallography, that this connectivity is apparently incorrect and that instead the disulfides form a different connectivity that shares two of the disulfides from the originally proposed connectivity, 7-23 and 11-19, but the vicinal disulfide is absent, and the other two disulfide bonds are located between 10-13 and 14-22 (Jordan, et al., 2009). In this structure hepcidin forms a β-hairpin-like motif containing a central core cross-linked by disulfides and a flexible six residue N-terminal region. It was shown that at physiological temperature hepcidin interconverts between two conformations (Jordan, et al., 2009). NMR studies at lower and higher temperatures showed that the conformational variation occurs predominantly around the β-hairpin region of the peptide and that the N-terminal region is flexible at all temperatures. The physiological role, if any, of this conformational flexibility remains unclear.

Hepcidin is deactivated by cleavage of the N-terminal region of the molecule, as indicated by the presence of a 20 residue inactive form of hepcidin isolated from urine (Park, et al., 2001). The N-terminal region of hepcidin is essential for binding to ferroportin as sequential truncation of the N-terminal residues results in a progressive loss in activity of the peptide, yet the N-terminal region alone is not sufficient to induce ferroportin internalisation (Nemeth, et al., 2006). In addition, it has been shown that Cys326 of ferroportin is required for the interaction between hepcidin and ferroportin, which raises the possibility that, among other explanations, a disulfide bond might form between hepcidin and ferroportin (Fernandes, et al., 2009).

Hepcidin dysregulation results in a number of disease states. Haemochromatosis is a genetic condition characterised by abnormally high levels of circulating iron, resulting in iron deposition and subsequent organ damage (Alexander and Kowdley, 2009). Most forms of haemochromatosis result from a deficiency in hepcidin production and therefore it should be possible to treat haemochromatosis by administration of synthetic hepcidin or a hepcidin analogue. At the other extreme, in anemia of chronic disease associated with chronic infection or inflammation, high hepcidin levels limit the availability of iron for haemoglobin synthesis. Here antagonists of hepcidin might be therapeutically useful in correcting the iron imbalance.

A key element in the potential development of hepcidin-based treatments for iron regulatory disorders is an understanding of the structure/activity relationships of hepcidin and its interaction with ferroportin. In this study we undertake mutational studies on the N-terminal residues of hepcidin to elucidate these relationships. As our initial approach we performed an alanine scan to determine the specific residues within the N-terminus of hepcidin that are involved in its interaction with ferroportin. We subsequently explored the important structural and chemical features required at each of the key positions identified from the alanine scan to establish the structure/activity profile of the critical N-terminus of hepcidin. A series of selenocysteine mutants were also examined in an attempt to determine the role of disulfide exchange in the hepcidin/ferroportin interaction. These studies have provided a mechanistic insight into the binding mode of hepcidin with ferroportin.

Results

Peptide synthesis

The synthesis of the hepcidin analogues for the structure/activity studies was undertaken in two rounds. The first round involved the synthesis of a series of alanine mutants in which each residue of the N-terminal region was individually replaced with alanine. The second

round of analogues was based on bioactivity data (described below) and involved mutations of residues His3, Phe4 and Ile6. All analogues were successfully synthesised via solid phase synthesis methods utilising Fmoc chemistry. After assembly and cleavage from the resin using TFA, the peptides were oxidised in phosphate buffer containing guanidine, EDTA, cysteine and cystine to yield a complex mixture of disulfide isomers, as illustrated by the RP-HPLC trace of the crude oxidation mixture shown in Figure 2. Despite this complexity, we were able to isolate, in high purity, a major isomer for 24 of the 26 analogues synthesised (Figure 2). Each of these isomers was analysed by NMR spectroscopy to confirm that they possessed the native hepcidin fold. Two of the analogues synthesised, F9K and G20F, could not be successfully oxidised to a native-like molecule. These two mutations were originally chosen because of the high sequence conservation at these positions and their proximity to the N-terminal region, and therefore we believed that they might play a role in the biological activity of hepcidin. However, our results suggest that Phe9 and Gly20 might be conserved because they are important for the correct folding of hepcidin.

Six selenocysteine analogues of hepcidin were designed, i.e.[C7U,C23U]hepcidin, [C10U,C13U]hepcidin, [C11U,C19U]hepcidin, [C14U,C22U]hepcidin, [C7U,C10U,C13U,C23U]hepcidin (Sec_4) and [C7U,C10U,C11U,C13U,C14U,C19U,C22U,C23U]hepcidin (Sec_8), with the aim of elucidating the role of one or more of the disulfide bonds of hepcidin in a potential disulfide exchange with ferroportin. Due to the low pKa and highly negative redox potential of selenocysteine the formation of a diselenide bond is favoured over a mixed selenylsulfide; furthermore diselenides are highly resistant to reduction by thiols (Armishaw, et al., 2006; Muttenthaler and Alewood, 2008). Therefore, if one of the hepcidin disulfide bonds underwent exchange with ferroportin, replacing it with a diselenide would result in a loss of activity as it would be unlikely to form a selenylsulfide bond with the free thiol of the ferroportin Cys326 residue. The selenocysteine analogues of hepcidin were synthesised by solid phase peptide synthesis using BOC chemistry. The peptides were cleaved from the resin using hydrofluoric acid, and during this process generated peptide in which the selenocysteines were oxidised as expected (Muttenthaler and Alewood, 2008). The remaining cysteines were then oxidised under the same conditions used for the structure/activity analogues. Interestingly, the [Sec_8]hepcidin analogue, in which all the cysteines are replaced with selenocysteine, folded into a single major oxidised product in hydrofluoric acid during the resin cleavage reaction that was subsequently shown by NMR to be the native isomer. The peptides were then purified by RP-HPLC and by NMR to confirm that they were correctly folded.

NMR Studies

NMR spectroscopy was used to confirm that the hepcidin analogues all possessed a native fold. NH_i-NH_{i+1}, αH_i-NH_{i+1} and βH_i-NH_{i+1} connectivities obtained from the NOESY spectrum for each analogue were used in the sequential assignment of individual spin systems determined from the TOCSY spectrum. Sequential αH_i-NH_{i+1} connectivities were seen for the entire peptide chain except for residues 14 to 15, which were not visible in the spectra, and at Pro5. The absence of residues Cys14 and His15 is consistent with a similar observation for the native peptide (Hunter, et al., 2002; Jordan, et al., 2009). The presence of αH_i-δH_{i+1} NOE correlations indicated that Pro5 was in a *trans* configuration in all analogues.

Secondary αH chemical shifts are the difference between an observed αH chemical shift and that of the corresponding residue in a random coil peptide. A comparison of secondary αH shifts between different peptides provides information on the similarity of their structures. Furthermore, an analysis of secondary shift data yields information on the secondary structures present within peptides. Figure 3 shows a comparison between the secondary αH

chemical shifts of the six alanine mutants and native hepcidin and highlights the structural similarity between these peptides. Only small local variations in secondary shifts are observed in the N-terminal region around the sites of amino acid substitution in each analogue. The trends in shifts for the core of the molecule, which is defined by the cystine framework, are almost identical, including a series of positive secondary shift values from residues 6 to 11 and 17 to 24, consistent with the proposed β-hairpin structure of hepcidin. Similar results were observed for the structural analysis of the position 3, 4 and 6 analogues and the selenocystine analogues (see Supplementary Figure 1). Therefore any changes in biological activity observed are likely to be due to changes in the chemical characteristics of the specific amino acids and not a change in the global structure of the peptides.

Bioactivity of the hepcidin analogues

The ability of the hepcidin analogues to induce ferroportin internalisation and degradation was assessed by a measurement of the suppression of fluorescence in HEK cells expressing ferroportin-GFP. Peptides (0.3 μM) were added to the cells and the activity of each mutant expressed as a percentage of native hepcidin activity (Table 1). The initial screening was performed on the alanine mutants to characterise the effect of mutation of each individual amino acid of the N-terminus on activity of the peptide (Figure 4A). Mutation of residues Thr2 to alanine resulted in no significant change in activity compared with native hepcidin, with suppression of fluorescence relative to hepcidin of 88 ± 13%. A moderate loss in activity was observed on mutation of Asp1 (68 ± 5%) and Pro5 (77 ± 3%) to alanine. The largest effect was seen when His3, Phe4 or Ile6 were changed to alanine, with these mutants having only 49 ± 1%, 33 ± 18% and 31 ± 4%, respectively, of the activity of native hepcidin. Therefore, the key residues identified by the alanine scan for the interaction between hepcidin and ferroportin are His3, Phe4 and Ile6.

A second series of analogues was then made to elucidate the specific chemical requirements at each of these positions required for binding of hepcidin to ferroportin (Figure 4B-D). None of the three positions tolerated the presence of positively or negatively charged residues, as substitution of lysine or aspartic acid at any of these positions resulted in almost complete loss in activity. At position 3 (Figure 4B), substitution of the histidine with a phenylalanine ring resulted in an almost fully active peptide (92 ± 0.3%), suggesting that the nitrogens in the histidine ring are not required for interaction with the receptor. A tryptophan at position 3 resulted in a substantial loss of activity (56 ± 5%), presumably due to the greater bulk of this residue. Changing the stereochemistry by incorporation of a D-histidine resulted in some loss in activity (73 ± 2%), which suggests that although the sidechain orientation of this residue has some effect, either ferroportin can accommodate this change to some degree or the flexibility of the N-terminus can compensate for the change in stereochemistry. Replacement of Phe4 with a cyclohexylalanine or a norleucine resulted in little or no loss in activity (88 ± 8% and 105 ± 11%, respectively), indicating that neither an aromatic or ring moiety is required at this position and that a long hydrophobic sidechain is sufficient for activity (Figure 4C). This suggestion is further supported by the data associated with the introduction of a more polar residue, tyrosine, which causes some loss of activity (75 ± 22%). The interaction is also stereospecific because substitution with D-phenylalanine results in a peptide with an activity of only 29 ± 15% relative to hepcidin. Substitution of Ile6 with a phenylalanine leads to a loss in activity (64 ± 4%), suggesting that a bulkier aromatic ring at this position cannot be accommodated by ferroportin as easily as the branched isoleucine (Figure 4D). Mutation to a D-isoleucine also results in a loss of activity (55 ± 2%), implying that there is a stereochemical preference for the interaction.

Because the interaction between hepcidin and ferroportin appeared to be dominated by hydrophobic interactions two additional mutants were synthesised, with Pro5 altered to a hydroxyproline and the highly conserved Ile8 and Phe9 residues to a lysine. Neither the

mutation of Pro5 to hydroxyproline or Ile8 to lysine resulted in any substantial loss of hepcidin activity (Table 1). As stated earlier, we were unable to produce a correctly folded F9K mutant.

To examine the role of the disulfide bonds in the interaction between hepcidin and ferroportin, a series of selenocysteine analogues of hepcidin were synthesised and tested for their ability to induce ferroportin internalisation and degradation (Figure 5A). Interestingly, all of the diselenide analogues exhibited an almost identical dose-response curve to hepcidin (Figure 5B), suggesting that a thiol exchange between hepcidin and ferroportin is not essential for hepcidin activity. However, reduction/alkylation assays on native and Sec_8 hepcidin revealed that although [Sec_8]hepcidin was more stable to reduction by DTT than native hepcidin, the peptide could still be reduced (Figure S2). Interestingly, if the reaction time was extended, [Sec8]hepcidin was found to reoxidise, presumably due to exhaustion of DTT in the reaction.

Antagonists of hepcidin have the potential to be used as a treatment for anaemia of inflammation, an iron deficiency disease that results from chronic over production of hepcidin. Therefore, the less active mutants synthesised in this study were tested for their ability to act as antagonists of native hepcidin. None of the hepcidin analogues exhibited antagonistic activity against the action of hepcidin in the ferroportin-GFP assay when hepcidin and each analogue were co-incubated (data not shown).

Discussion

In this study we have characterised the key N-terminal residues of hepcidin involved in its interaction with ferroportin. Figure 6A summarises the structure/activity data known for hepcidin from natural mutations (Biasiotto, et al., 2003; Jacolot, et al., 2004; Merryweather-Clarke, et al., 2003; Nemeth, et al., 2006), previous studies (Nemeth, et al., 2006; Nemeth, et al., 2004) and this work. Substitution of His3, Phe4 or Ile6 with alanine resulted in a substantial loss in the ability of the hepcidin mutants to trigger the internalisation and degradation of ferroportin. More extensive substitutions at each of these positions revealed that the interaction between hepcidin and ferroportin is dominated by hydrophobic interactions, because mutation of any of the identified residues in hepcidin with charged amino acids resulted in a complete loss of activity. Finally, a change in stereochemistry of Phe4 and Ile6 by substitution with the corresponding D-amino acid caused a significant loss of activity. This suggests that these interactions are also stereospecific.

Figure 6B maps the structure/activity data onto the molecular surface of hepcidin. It can clearly be seen that His3, Phe4 and Ile6 form a localised patch at one end of the molecule and that this patch is flanked by the other N-terminal residues that have a small to moderate influence on activity. The known natural hepcidin mutant, G21D, and the synthetic mutant, M21Y, exhibit comparable activity to native hepcidin (Nemeth, et al., 2006). Based on the data obtained from this study and truncations of the N-terminus (Nemeth, et al., 2006), this finding is not surprising as both these residues are located at the opposite end of the molecule to the activity hotspot. The importance of the N-terminal residues in the interaction of hepcidin with ferroportin is further highlighted by a comparison of mammalian hepcidin sequences. Figure 6C illustrates the fact that the N-terminal residues important for biological activity are among the most highly conserved, whereas residues located away from the activity centre, around the β-turn, are less conserved.

The extracellular loop of ferroportin that interacts with hepcidin has recently been identified from the observation that Cys326 mutation in this loop result in ferroportin being resistant to hepcidin binding (De Domenico, et al., 2005; Fernandes, et al., 2009). It has been proposed

that the free thiol of the Cys326 residue forms a disulfide bond with one of the cysteine residues in hepcidin (Fernandes, et al., 2009). We attempted to test this hypothesis by synthesising a series of diselenide bond mutants of hepcidin. Diselenide bonds are structurally analogous to disulfide bonds but are more resistant to reduction (Armishaw, et al., 2006; Muttenthaler and Alewood, 2008) and therefore we envisaged that if a hepcidin disulfide bond was involved in a disulfide exchange with ferroportin replacement of this bond with a diselenide would result in a loss of activity. Diselenide analogues were designed to test the effects of replacing both individual and multiple disulfide bonds and all peptides were shown to be structurally comparable by NMR secondary shift analysis. This analysis also confirmed the recently revised disulfide connectivity and three dimensional structure of hepcidin, as the [C10U,C13U]hepcidin and [C14U,C22U]hepcidin analogues had identical secondary shifts to native hepcidin (Jordan, et al., 2009). Activity assays revealed that the activity of all the diselenide analogues was comparable to native hepcidin, suggesting that no disulfide exchange occurs between the hepcidin and receptor. However, in reduction trials we found that it was possible to reduce [Sec_8]hepcidin with DTT and therefore the occurrence of disulfide exchange between hepcidin and ferroportin cannot be unequivocally resolved.

None of the hepcidin analogues exhibited enhanced activity compared with native hepcidin, a finding that might be due to one of several reasons. Firstly, the ferroportin-GFP degradation assay used is designed to give maximal degradation of ferroportin-GFP when incubated with native hepcidin and therefore might only detect mutants with decreased activity. Also, the native hepcidin sequence might be optimised for its interaction with ferroportin, which is supported by the high sequence conservation across species, and therefore the existing interactions are highly efficient. For example, in the case of Phe4 it appears that this interaction is simply a hydrophobic one that is relatively tolerant to size as long as the correct stereochemistry is maintained. Alternatively, single point mutations might not be sufficient to enhance activity significantly and multi-point mutation analogues might be needed to produce a more efficacious hepcidin analogue. Finally, it is also possible that there are mutations at these positions that could improve activity that were not synthesised in this study and that the incorporation of unnatural amino acids into the sequence of hepcidin and variation of non-critical amino acids to introduce additional contacts might be avenues to explore for the production of more potent hepcidin analogues.

Hepcidin has an exceptionally high cysteine content relative to other proteins (Fahey, et al., 1977), with 8 of the 25 residues being cysteine (~30%). When eight cysteines are present in a peptide there are 105 possible four-disulfide isomers that can be produced from a random oxidation. Therefore it is very surprising that it is possible to fold hepcidin *in vitro* into the native isomer, even in the denaturing conditions used in this study. In a stunning illustration of this robust folding, we observed that correctly folded [Sec_8]hepcidin was formed spontaneously during the hydrofluoric acid cleavage reaction. Presumably, there are interactions between residues within the sequence that drive the correct folding of hepcidin to favour the native disulfide connectivity. Our results show that the F9K and G20F mutations disrupted folding, suggesting that these changes to the hepcidin sequence introduce interactions unfavourable to formation of the native disulfide isomer.

It is interesting to consider what role the framework of hepcidin plays in its biological function, considering that many of the key residues important for biological activity are localised within the flexible N-terminus. It has been shown that the N-terminus alone is not sufficient for activity (Nemeth, et al., 2006), which implies a role for other residues within the framework. In addition to the conserved cysteines, which provide structural stability to the molecule and might form an intermolecular disulfide with ferroportin, there are a number of residues within the hepcidin sequence that are conserved across species (Figure

6C) and it is possible that these could be important for either the interaction of hepcidin with ferroportin or might modulate other processes in the internalisation mechanism.

Significance

Hepcidin is the major peptide hormone in the body regulating iron levels. There are a number of diseases associated with the disregulation of hepcidin levels in humans, including haemochromatosis (iron overload) and anaemia (low iron levels). This study represents a first step towards defining the hepcidin pharmacophore at the ferroportin binding site and the data generated could be crucial in the development of agonists or antagonists for the treatment of iron-related disorders. We have identified the key positions within the N-terminus of hepcidin for its ability to trigger internalisation and degradation of ferroportin and have elucidated the chemical and structural requirements at each of these positions. Our findings, combined with literature data, have allowed us to propose a mechanistic model for the hepcidin/ferroportin interaction that we can interrogate in future studies and will be invaluable in the drug development process.

Experimental Procedures

Peptide Synthesis

All peptides were assembled on 2-Cl-2-trityl resin (Novabiochem) by solid-phase peptide synthesis on a Liberty Microwave Peptide Synthesiser using the *in situ* neutralisation/HBTU protocol and Fmoc chemistry (Schnölzer, et al., 1992). Cleavage of the peptides from the resin was achieved using TFA with tri-isopropylsilane and water as scavengers (9:0.5:0.5 (v/v) TFA:tri-isopropylsilane:water) at 22°C for 2 h. The selenocysteine analogues of hepcidin were synthesised with the *in situ* neutralisation/HBTU protocol and Boc chemistry using Boc-Sec(MeBzl)-OH at sites where selenocysteine was replacing cysteine. These peptides were cleaved using HF with *p*-cresol and *p*-thiocresol as scavengers (9:0.5:0.5 (v/v) HF:*p*-cresol:*p*-thiocresol). The reaction was allowed to proceed at −5 to 0°C for 1.5 h. The HF was then removed under vacuum and the peptide precipitated with ether, filtered, dissolved in 50% acetonitrile containing 0.05% TFA and lyophilised. After cleavage, the peptide was precipitated with ether, filtered and then dissolved in 50% acetonitrile containing 0.05% TFA and lyophilised. Crude peptides were purified by RP-HPLC on a C_{18} column using a gradient of 0-80% B (A – H_2O/0.05% TFA, B – 90% CH_3CN/10% H_2O/0.045% TFA) in 80 min. Analytical RP-HPLC and ES-MS confirmed the purity and molecular mass of the synthesised peptides.

The reduced peptides were oxidised by incubating in 0.1 M sodium phosphate buffer containing 4 M guanidine, 2 mM EDTA, 3 mM cysteine and 0.15 mM cystine (pH 7.8) for approximately 18 h at room temperature. The reaction mixture was purified by RP-HPLC to yield the cyclic/oxidised peptides. Analytical RP-HPLC and ES-MS confirmed the purity of the final products. All hepcidin analogues were stored as lypholised solids at -20°C.

NMR studies

Structural data for the hepcidin analogues were obtained using NMR spectroscopy for samples dissolved in 90% H_2O and 10% D_2O at a pH of approximately 4. A Bruker Avance 600 MHz NMR spectrometer was used to acquire spectra, including ^1H, TOCSY and NOESY data, as described previously (Clark, et al., 2006; Clark, et al., 2006) and processed using Topspin (Bruker). All spectra were recorded at 298 K. Processed spectra were analysed and assigned within the program Sparky (Goddard and Kneller, 2008).

Flow cytometry

ECR293-Fpn, a cell line stably transfected with the mouse ferroportin-GFP construct under the control of ponasterone-inducible promoter, was prepared and maintained as described previously (Nemeth, et al., 2004). Briefly, cells expressing Fpn-GFP were treated with peptides (0.3 μM) for 24 h. Peptide concentrations were determined by measurement of absorbance at 214 nm and using a calculated extinction coefficient based on the peptide sequence (Moffatt, et al., 2000). Cells not induced with ponasterone to express Fpn-GFP were used to establish a gate to exclude background fluorescence and cells induced with ponasterone, but not treated with peptides, were used as the positive control. After treatment with hepcidin or its mutated analogues (n = 3 - 6) the cells lost fluorescence in proportion to the activity of each peptide. The results were expressed as a fraction of the activity of hepcidin, according to the formula $1 - [(F_x - F_{hep25}) / (F_{untreated} - F_{hep25})]$, where F was the mean fraction of cells within the green fluorescence gate and x was the peptide.

Antagonist competition of hepcidin

ECR293-Fpn, a cell line stably transfected with the mouse ferroportin-GFP construct under the control of ponasterone-inducible promoter, was prepared and maintained as described previously (Nemeth, et al., 2004). Briefly, cells expressing Fpn-GFP were treated with Hep25 (0.717 μM) and with mutant (3.3 – 3.6 μM) simultaneously for 24 h.

Supplementary Material

Refer to Web version on PubMed Central for supplementary material.

Acknowledgments

Work in our laboratory on hepcidin is supported by a grant from the National Health and Medical Research Council (NHMRC, ID456073). DJC is a NHMRC Principal Research Fellow. RJC is a NHMRC Biomedical Career Development Award Fellow. We gratefully acknowledge access to the facilities of the ARC Special Research Centre for Functional and Applied Genomics. Work in the Los Angeles laboratory was supported by NIH grants R01 DK082717 and R01 DK 065029 (TG, EN and GP).

References

Alexander J, Kowdley KV. HFE-associated hereditary hemochromatosis. Genet Med. 2009; 11:307–313. [PubMed: 19444013]

Armishaw CJ, Daly NL, Nevin ST, Adams DJ, Craik DJ, Alewood PF. Alpha-selenoconotoxins, a new class of potent alpha7 neuronal nicotinic receptor antagonists. J Biol Chem. 2006; 281:14136–14143. [PubMed: 16500898]

Biasiotto G, Belloli S, Ruggeri G, Zanella I, Gerardi G, Corrado M, Gobbi E, Albertini A, Arosio P. Identification of new mutations of the HFE, hepcidin, and transferrin receptor 2 genes by denaturing HPLC analysis of individuals with biochemical indications of iron overload. Clin Chem. 2003; 49:1981–1988. [PubMed: 14633868]

Clark RJ, Daly NL, Craik DJ. Structural plasticity of the cyclic-cystine-knot framework: implications for biological activity and drug design. Biochem J. 2006; 394:85–93. [PubMed: 16300479]

Clark RJ, Fischer H, Nevin ST, Adams DJ, Craik DJ. The synthesis, structural characterization, and receptor specificity of the alpha-conotoxin Vc1.1. J Biol Chem. 2006; 281:23254–23263. [PubMed: 16754662]

De Domenico I, Ward DM, Nemeth E, Vaughn MB, Musci G, Ganz T, Kaplan J. The molecular basis of ferroportin-linked hemochromatosis. Proc Natl Acad Sci U S A. 2005; 102:8955–8960. [PubMed: 15956209]

Donovan A, Lima CA, Pinkus JL, Pinkus GS, Zon LI, Robine S, Andrews NC. The iron exporter ferroportin/Slc40a1 is essential for iron homeostasis. Cell metabolism. 2005; 1:191–200. [PubMed: 16054062]

Fahey RC, Hunt JS, Windham GC. Cysteine and Cystine Content of Proteins - Differences between Intracellular and Extracellular Proteins. Journal of Molecular Evolution. 1977; 10:155–160. [PubMed: 592421]

Fernandes A, Preza GC, Phung Y, De Domenico I, Kaplan J, Ganz T, Nemeth E. The molecular basis of hepcidin-resistant hereditary hemochromatosis. Blood. 2009; 114:437–443. [PubMed: 19383972]

Ganz T. Iron homeostasis: fitting the puzzle pieces together. Cell metabolism. 2008; 7:288–290. [PubMed: 18396134]

Goddard, TD.; Kneller, DG. SPARKY 3. University of California; San Francisco:

Hunter HN, Fulton DB, Ganz T, Vogel HJ. The solution structure of human hepcidin, a peptide hormone with antimicrobial activity that is involved in iron uptake and hereditary hemochromatosis. J Biol Chem. 2002; 277:37597–37603. [PubMed: 12138110]

Jacolot S, Le Gac G, Scotet V, Quere I, Mura C, Ferec C. HAMP as a modifier gene that increases the phenotypic expression of the HFE pC282Y homozygous genotype. Blood. 2004; 103:2835–2840. [PubMed: 14670915]

Jordan JB, Poppe L, Haniu M, Arvedson T, Syed R, Li V, Kohno H, Kim H, Schnier PD, Harvey TS, et al. Hepcidin revisited, disulfide connectivity, dynamics, and structure. J Biol Chem. 2009; 284:24155–24167. [PubMed: 19553669]

Krause A, Neitz S, Magert HJ, Schulz A, Forssmann WG, Schulz-Knappe P, Adermann K. LEAP-1, a novel highly disulfide-bonded human peptide, exhibits antimicrobial activity. FEBS Lett. 2000; 480:147–150. [PubMed: 11034317]

Lauth X, Babon JJ, Stannard JA, Singh S, Nizet V, Carlberg JM, Ostland VE, Pennington MW, Norton RS, Westerman ME. Bass hepcidin synthesis, solution structure, antimicrobial activities and synergism, and in vivo hepatic response to bacterial infections. J Biol Chem. 2005; 280:9272–9282. [PubMed: 15546886]

Merryweather-Clarke AT, Cadet E, Bomford A, Capron D, Viprakasit V, Miller A, McHugh PJ, Chapman RW, Pointon JJ, Wimhurst VL, et al. Digenic inheritance of mutations in HAMP and HFE results in different types of haemochromatosis. Hum Mol Genet. 2003; 12:2241–2247. [PubMed: 12915468]

Moffatt F, Senkans P, Ricketts D. Approaches towards the quantitative analysis of peptides and proteins by reversed-phase high-performance liquid chromatography in the absence of a pure reference sample. Journal of Chromatography A. 2000; 891:235–242. [PubMed: 11043783]

Muttenthaler M, Alewood PF. Seleonpeptide Chemistry. J Pept Sci. 2008; 14:1223–1230. [PubMed: 18951416]

Nemeth E, Ganz T. Regulation of iron metabolism by hepcidin. Annu Rev Nutr. 2006; 26:323–342. [PubMed: 16848710]

Nemeth E, Preza GC, Jung CL, Kaplan J, Waring AJ, Ganz T. The N-terminus of hepcidin is essential for its interaction with ferroportin: structure-function study. Blood. 2006; 107:328–333. [PubMed: 16141345]

Nemeth E, Tuttle MS, Powelson J, Vaughn MB, Donovan A, Ward DM, Ganz T, Kaplan J. Hepcidin regulates cellular iron efflux by binding to ferroportin and inducing its internalization. Science. 2004; 306:2090–2093. [PubMed: 15514116]

Park CH, Valore EV, Waring AJ, Ganz T. Hepcidin, a urinary antimicrobial peptide synthesized in the liver. J Biol Chem. 2001; 276:7806–7810. [PubMed: 11113131]

Schneider TD, Stephens RM. Sequence logos: a new way to display consensus sequences. Nucleic Acids Res. 1990; 18:6097–6100. [PubMed: 2172928]

Schnölzer M, Alewood P, Jones A, Alewood D, Kent SBH. *In situ* neutralization in Boc-chemistry solid phase peptide synthesis. Int J Pept Protein Res. 1992; 40:180–193. [PubMed: 1478777]

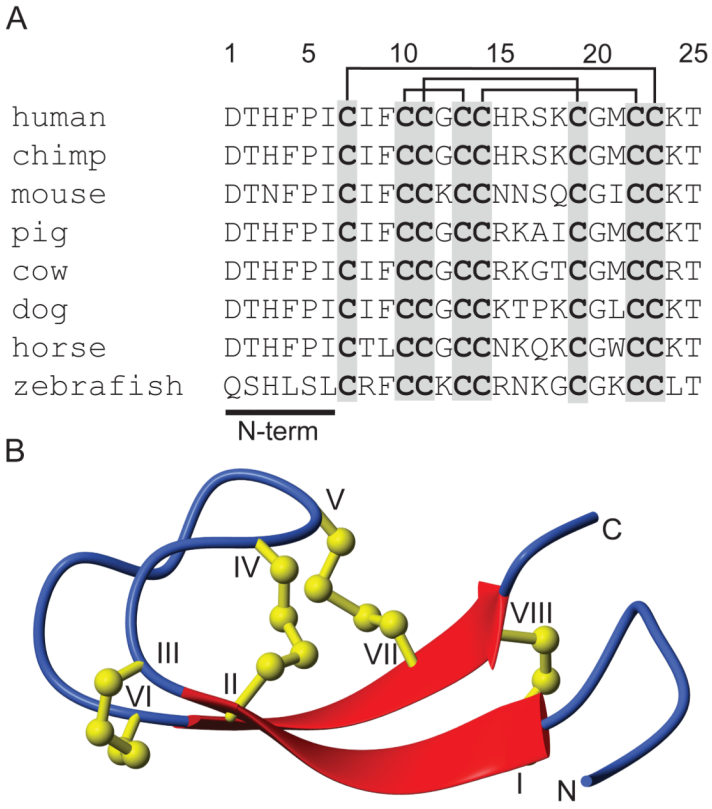

Figure 1.

Sequences and three-dimensional structure of hepcidin. (A). Sequence alignment of selected hepcidin sequences illustrating the high sequence conservation and the N-terminal region essential for biological activity. The sequences contain eight conserved cysteines that form four disulfide bonds, indicated by the lines above the sequence list. (B). A ribbon depiction of the three-dimensional structure of hepcidin showing the β-sheet structure (broad arrows) and the four disulfide bonds (ball and sticks).

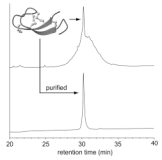

Figure 2.
Oxidation and purification of the hepcidin analogues. Oxidation of the reduced hepcidin analogues results in a complex mixture of disulfide isomers, but typically with one predominant species (top). This major isomer for each analogue was successfully purified by RP-HPLC (bottom) ready for structural analysis by NMR and bioactivity assays. The example shown is for the I6K mutant.

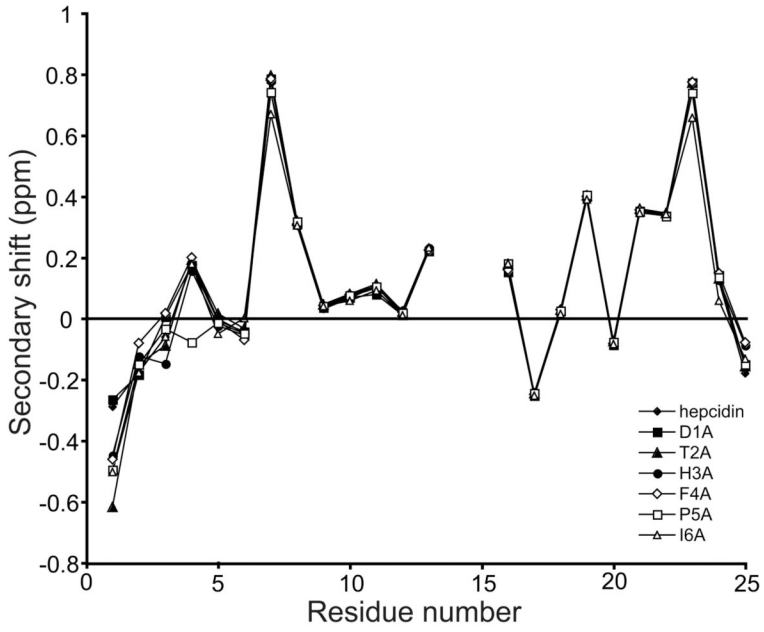

Figure 3.

NMR secondary shift analysis of the alanine mutants of hepcidin. All alanine mutants had almost identical αH secondary shift values to native hepcidin except for very small local changes around the site of substitution. A similar trend was observed for all the other hepcidin mutants analysed in this study (Figure S1).

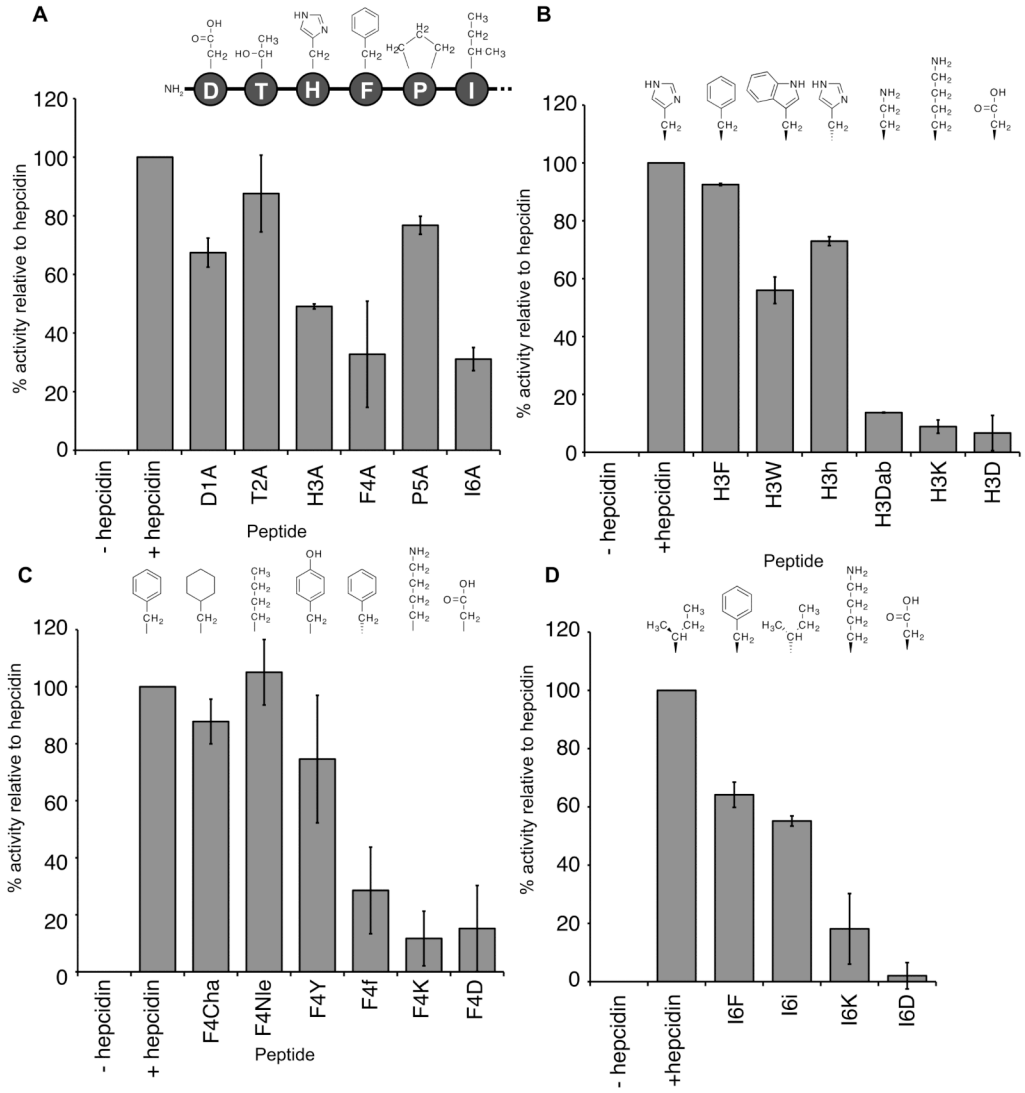

Figure 4.

Relative activities of native hepcidin and the alanine mutants (A), His3 mutants (B), Phe4 mutants (C) and Ile6 mutants (D). HEK293T cells stably expressing ferroportin-GFP construct were treated with peptide (0.3 μM) for 24 h and the intensity of green fluorescence was then measured by FACS and expressed as a percentage relative to native hepcidin.

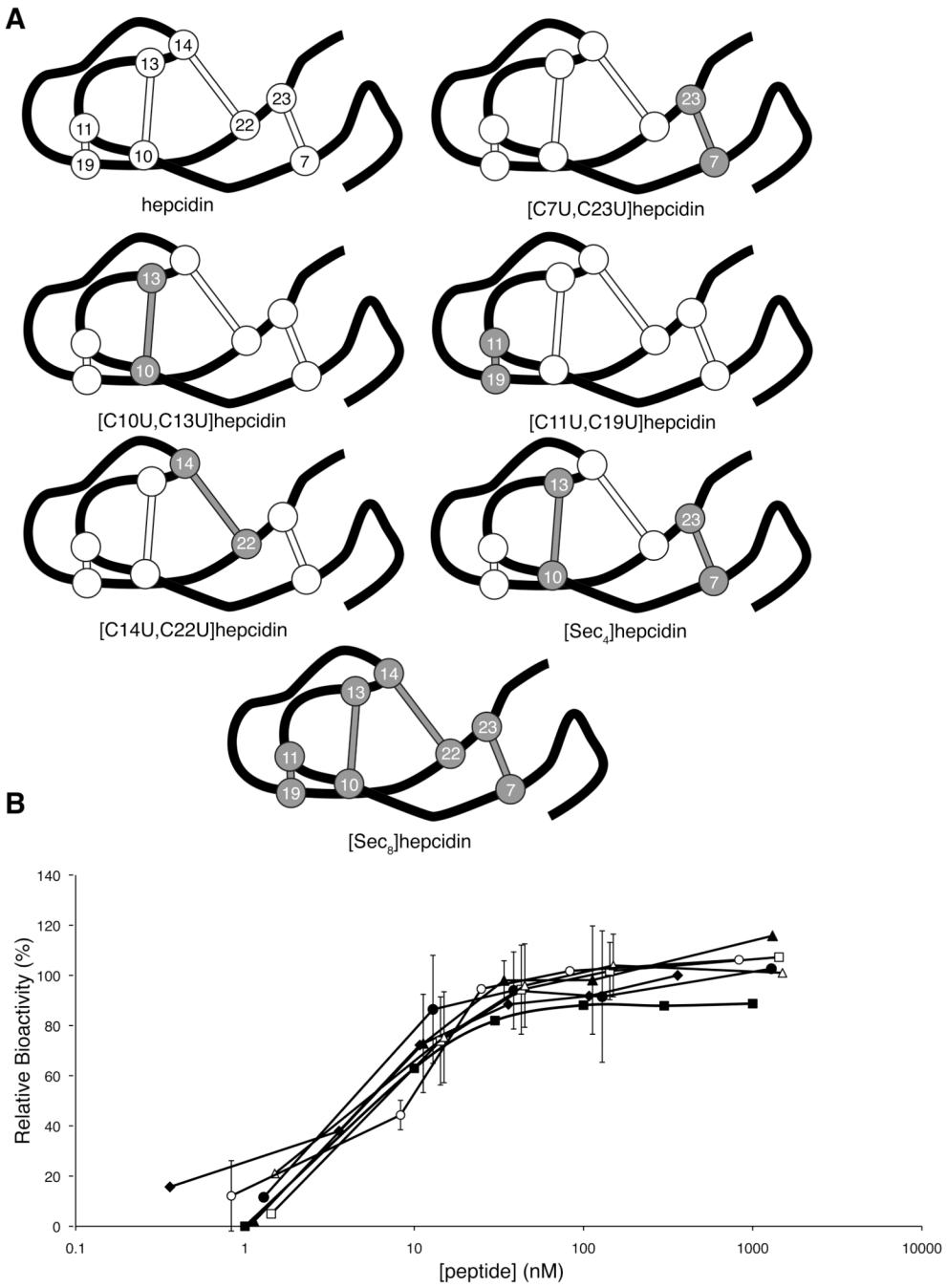

Figure 5.

Selenocystine analogues of hepcidin. (A) Schematic representation of native hepcidin and the selenocystine analogues synthesised in this study. The peptide backbone is represented by the black line, disulfides as white ball and sticks and diselenides and gray ball and sticks. Each disulfide/diselenide is numbered based on its position in the sequence. (B) Dose-response curve for hepcidin (filled diamonds), [U7C,U23C]hepcidin (filled squares), [C10U,C13U]hepcidin (filled triangles), [C11U,C19U]hepcidin (filled circles), [C14U, C22U]hepcidin (open squares), [Sec_4]hepcidin (open triangles) and [Sec_8]hepcidin (open circles). HEK293T cells stably expressing ferroportin-GFP construct were treated with

varying concentrations of peptide for 24 h and the intensity of green fluorescence was then measured by FACS. See also Figure S2.

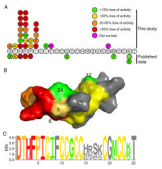

Figure 6.

Summary of structure/activity relationships of hepcidin. (A). The sequence of hepcidin showing the effect on activity of mutations from this study, naturally occurring mutations and truncation of the N-terminal residues (indicated by the X symbol) (Nemeth, et al., 2006). The colours indicate the percentage loss in activity relative to hepcidin as follows: green <10% loss in activity; yellow 10-20% loss; orange 20-50% loss; red >50% loss. Mutations shown in magenta are peptides that did not fold. (B). A surface representation of hepcidin with the surface colour-coded using the same scheme as panel A. The activity data presented is for the alanine mutants plus the known natural mutations. It can be seen that residues His3, Phe4 and Ile6 form a localised patch on the surface of the molecule. The conserved cysteines are coloured yellow. (C). A sequence logo representation (Schneider and Stephens, 1990) of hepcidin, coloured using the scheme from panel *A*. The activity data presented is for the alanine mutants together with the known natural mutations and the C-terminal truncation data (Nemeth, et al., 2006). The relative heights of the amino acids symbols at each position represent the degree of sequence conservation at each of these positions. As expected, the residues towards the N-terminal region of the peptide that are important for the interaction of hepcidin are the most highly conserved whereas those around the β-turn show lower sequence conservation.

Table 1

Bioactivity data for hepcidin analogues relative to native hepcidin.[a]

Peptide	% activity relative to hepcidin ± SEM[b]
hepcidin	100
D1A	67 ± 5
T2A	88 ± 13
H3A	49 ± 1
F4A	33 ± 18
P5A	77 ± 3
I6A	31 ± 4
H3F	92 ± 0.3
H3W	56 ± 5
H3h	73 ± 2
H3Dab[c]	14 ± 0.1
H3K	9 ± 2
H3D	7 ± 6
F4Cha[d]	88 ± 8
F4Nle[e]	105 ± 11
F4Y	75 ± 22
F4f	29 ± 15
F4K	15 ± 15
F4D	12 ± 10
I6F	64 ± 4
I6i	55 ± 2
I6K	18 ± 12
I6D	2 ± 5
I8K	87 ± 5
P5O[f]	89 ± 2

[a] Activity relative to native hepcidin using the GFP-ferroportin assay.

[b] $n = 3 - 6$

[c] diaminobutyric acid.

[d] cyclohexylalanine.

[e] norleucine.

[f] hydroxyproline